

PAPER • OPEN ACCESS

## Brief review on cathodoluminescence application in solid-state devices

To cite this article: M.E Emeteri *et al* 2019 *J. Phys.: Conf. Ser.* **1378** 022023

View the [article online](#) for updates and enhancements.



**IOP | ebooks™**

Bringing together innovative digital publishing with leading authors from the global scientific community.

Start exploring the collection—download the first chapter of every title for free.

## Brief review on the physics of solid-state lighting device

Emetere M.E.,<sup>1,2</sup>, Abodunrin J.T.<sup>1</sup>, Fayomi O.O.<sup>3</sup>, Iroham C.O.<sup>4</sup>

<sup>1</sup>Physics Department, Covenant University, Ota- Nigeria

<sup>2</sup>Department of Mechanical Engineering Science, University of Johannesburg, South Africa.

<sup>3</sup>Department of Political Science and International Relations, Covenant University, Ota, Nigeria

<sup>4</sup>Department of Estate Management, Covenant University, Ota, Nigeria  
emetere@yahoo.com

### Abstract-

In this review, the chronological advances of solid state lighting (SSL) alongside the theoretical predictions was examined. The discussion includes its crystallographic orientations, substrate growth, colour rendering, misfit dislocations, quantum well fabrication, stacking fault and energy efficiency. It has been discovered that the challenges confronting the potential of SSL devices may not just be ambient temperature of the operating environment or the safe limits of the blue/white-light hazard. This paper sheds lighter on the physics responsible for the SSL white lighting, wave function lapping at different crystallographic orientations and stress relaxation limits of quantum well (QW) heterointerfaces.

**Key words:** solid state lighting; light emitting diode; substrate growth; crystallographic orientations; semiconducting device; commercial white LED

### 1. Introduction

Solid state lighting (SSL) refers to a type of lighting that uses semiconductor light-emitting diodes (LEDs), organic light-emitting diodes (OLED), or polymer light-emitting diodes (PLED) as sources of illumination, rather than electrical filaments, plasma or gas. Oleg Vladimirovich Losev discovered the first LED in 1927. In 1962, Nick Holonyak, Jr., invented the first visible-spectrum LED in the form of red diodes. The advantages of the light-emitting diode (LED) or the Infrared emitting diode (IRED) over other known electronics lighting sources are low power requirement, high efficiency and long life. The successes recorded in solid-state lighting are beyond mere recombination of electron – hole pair or the activation of the p-n junction voltage. Over the years, scientists have propounded interesting concepts on the solid-state lighting that span from the chemistry of the materials to the quantum-mechanical behavior of its material [1-3].

In this paper, the LED was the main focus. One of the salient successes of the LED is the white light LED. White light LEDs are basically obtained from the phosphor down –conversion (PDC) method. PDC is achieved by using phosphor to obtain a redshift from short wavelengths or using blue InGaN LED to excite a yellow yttrium aluminum garnet (YAG) phosphor. This principle is adopted for the production of white light via mixing red, green, and blue phosphors with near-ultraviolet/ultraviolet (nUV/UV) InGaN diode chips [4]. The colour mixing approach is the mixing of phosphor with quantum wells (QWs) or varying layers of QDs e.g. blue-emitting QW at the top of the yellow-emitting QWs [5]. QWs are referred as potential wells



with discrete energy values. QDs selection during colour mixing depends on the output photoluminescence spectra and definite wavelength. Colour mixing technologies are recently applied to maximise the application of multi-colour and single colour LEDs in colour-controlled system.

SSL procedures or processes have its drawback. For example, the colour mixing approach still has drawback as regards its complex circuitry control and thermal variations within LEDs. The phosphor down-conversion method has challenges on its low efficiency, complex packaging, Stokes' shift energy loss and short lifetime due to degeneration of phosphor material [6]. These challenges shall be discussed in this review. Section 2 examines the ab-initio faults on the theories of the light emitting diode (LED). The misinterpretation of the LED theories was highlighted in section 3. In section 4, LED-growing techniques as it relates to the misleading theoretical predictions was discussed. In section 5, the complexities of the white LED and the unresolved theories were examined.

## 2. Ab-initio Faults about the Light Emitting Diode

Polar LED refers to the c-plane conventional LEDs whose spontaneous polarization is highest along the (0001) plane. Semi-polar LEDs refer to planes that restricts the inclination angles within  $0^\circ < \theta < 90^\circ$  in the (0001) plane and simultaneously reduces spontaneous polarization. Non-polar LEDs refer to planes perpendicular to the polar plane. In crystallographic point of view, polar planes emerge as a result of unequal number of constituents or atoms (e.g. N atoms and Ga atoms for GaN) in the double/mono layer plane. Hence, it occurs when the h,k,l in the plane of interest (h, k, i, l) is equal to zero e.g (0001). It is a semi-polar plane when h or k in the plane of interest is non-zero e.g. (1011). It is non-polar when 'l' in the plane of interest is equal to zero e.g. (1010) or (1110). In other words, the inclination angle, as well as the crystallographic orientation of interest is important to understand the corresponding properties of a particular plane (Figure 1 a & b). The semi-polar and nonpolar structures are known to reduce or eliminate polarization field. This is a positive step to improve upon LED efficiencies.

Also, non-polar or semipolar plane substrates can be obtained from polar plane e.g. non-polar m-plane (10 $\bar{1}$ 0) and semipolar plane substrates (11 $\bar{2}$ 2) and (10 $\bar{1}$ 1) are obtained by slicing a bulk GaN crystal [7].

In the initial theories of light emitting diode i.e. expressed in the Figure 2 below, when voltage is applied at the junction, electrons from the n-side migrates into the p-side. The migration of hole from the p-side to n-side is very minute; hence, the flow of electrons into the p-side is the primary source of current generation. In other words, migrating electrons (shown in Figure 2) are injected into the p-side to recombine with the holes to give a spontaneous emission of photons (light). This effect is called electroluminescence. In disordered structures, the electrons and holes are constrained; hence, it may possess a strong spatially correlated state in the form of excitons [8]. This concept is not always valid because of variation in the application of the disorder potential. The disordered potential distributions were theoretically calculated via solving the Schrodinger-Poisson equations [9]. However, the practical challenges of the

disordered potential still exist in the fabrication of high efficient devices. The resulting effect of the disordered potential is christened 'droop effect' [10]. The droop effect causes the efficiency of conventional light-emitting diodes (LEDs) grown on the polar c-plane to drop dramatically at high current densities. This effect is possible because the c-plane of InGaN/GaN is normal to the growth direction; hence, there is no shear stress along the c-plane [11]. The droop effect that is common at the c-plane of InGaN/GaN extends to thin quantum wells [12]. Practically, complex structures (e.g. InGaN/GaN) multiple-quantum-wells (MQWs) were utilized to reduce the droop effect but yielded low results due to carrier transport, non-uniform carrier distributions in the wells [13].

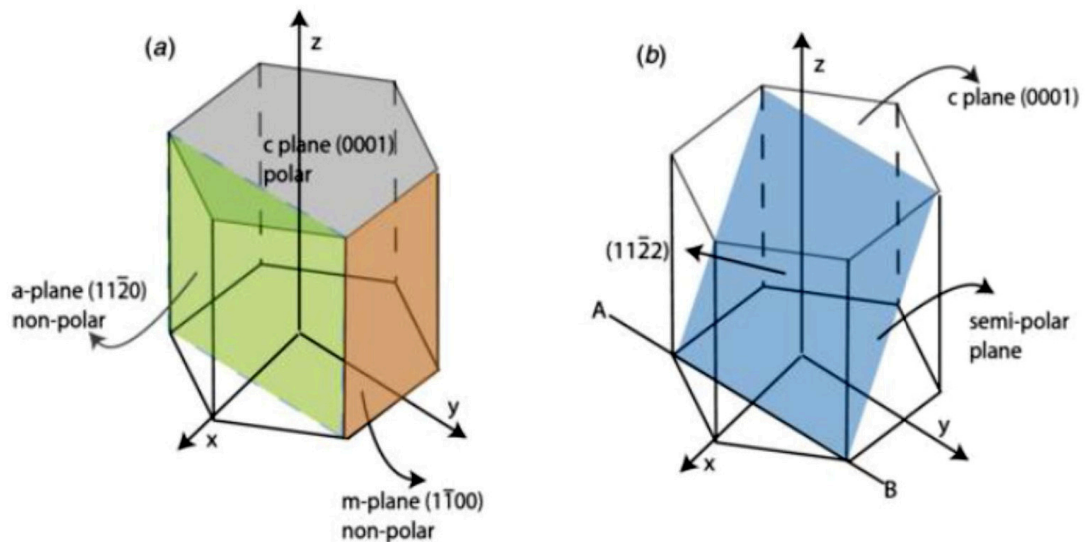


Figure 1: crystallographic orientation of interest (a) showing polar and non-polar plane (b) showing polar and semi-polar plane [14].

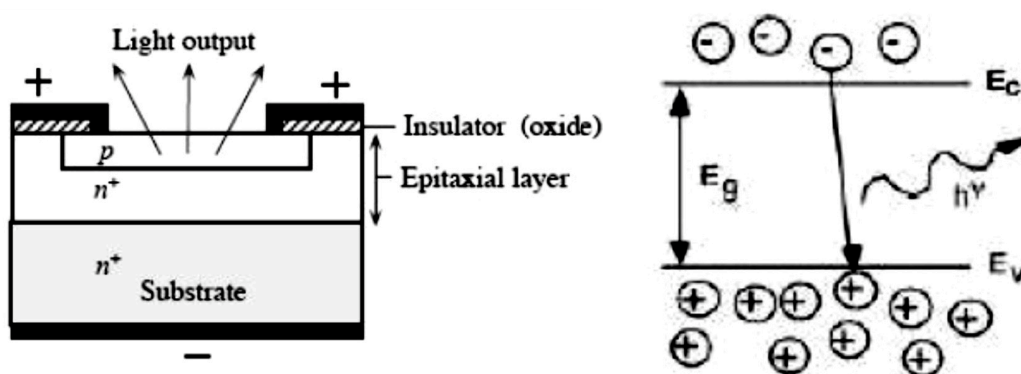


Figure 2: Electron-hole recombination in LED

Ref [15] solved numerically electron-hole recombination rate equations to determine the uncorrelated electrons and holes in quantum wells, hence, revealed the multi-faceted challenges in the LED quantum well (Figure 3). First, the wave function overlap (due to electrons in conduction and holes in valence bands) as a function of tilt angle with respect to the c-direction as shown in Figure 3a. This specific challenge leads to a large ( $>1$  MV/cm) electrostatic fields as shown in the later end of Figure 3a (decreased localization length), thereby reducing radiative recombination rates and efficiency. Then the quantum well (QW) active regions of InGaN LEDs was controlled with emphasis on the increased localization length and quantum size effects in disordered systems (Figure 3b). At increased localization length (Figure 3b) there is the tendency of obtaining high densities of extended defects, threading dislocations and stacking faults [16]. This theoretical prediction was found useful to fabricate a non-polar GaN template by heteroepitaxial growth on foreign substrates. Figure 3c examines the theoretical successes of combining quantum dots with quantum well to improve-on the low quality of the In-rich InGaN layers. The success of this prediction had been experimentally verified by Ref [17]. The negative downward energy transition rates in Figure 3d shows the tendency of wavelength-conversion loss in the phosphors as a results of the anomalies in the quantum well of the InGaN LEDs.

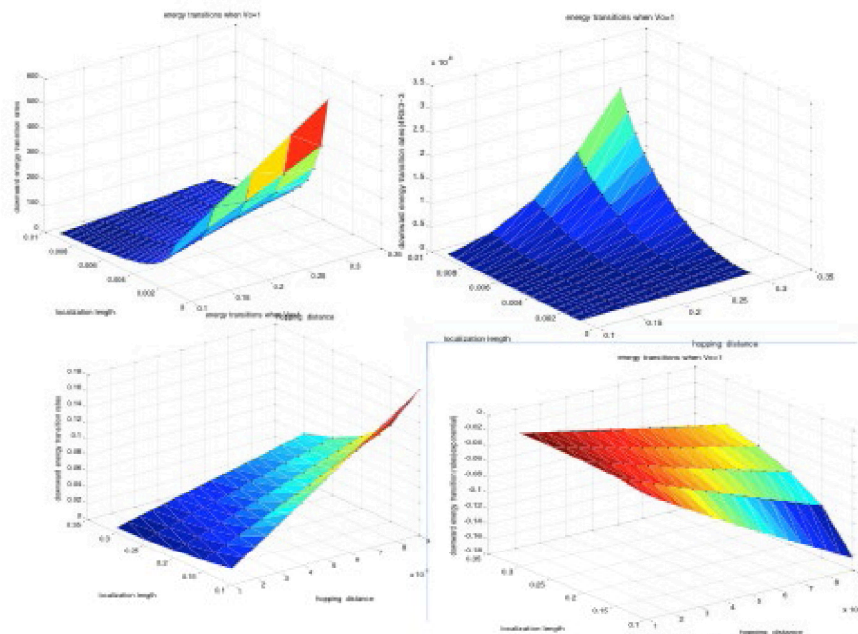


Figure 3: Challenges in the electron-hole recombination rate [15]. Z-axis is the downward energy transition rates, y-axis is the localization length and x-axis is the hopping distance

High-efficiency green and yellow semi-polar LEDs with an external quantum efficiency of 20.4% and 12.6% were used to obtain pure green LED at the 2021-plane [18-19]. However, this results is not valid for LED whose emission wavelength is lesser than 400 nm e.g. non-polar LEDs. Further in Figure 3, the active role of the impact ionization may not be caused by the energy developed by an electron/hole alone. Hardy et al., (2012) explained the variation noticed by Uno et al., [15] to be due to misfit dislocation (MD) noticed in the growth of high indium composition InGaN QWs. The misfit dislocation (MD) develops at the QW heterointerfaces due to stress relaxation processes [20] or strain relaxation caused by basal plane stacking faults (BPSFs) formation in the grown QW heterostructure [21-22].

Therefore, the challenges confronting the potentials of the solid state lighting device may not just be ambient temperature of the operating environment or exceeding the safe limits of the blue/white-light hazard. A fundamental error may still exist in its original experimental or theoretical representation.

### 3. Theoretical Misrepresentation of the Light Emitting Diode

The electron-hole recombination rates are subject to various intrinsic or extrinsic [23-24]. Recently, Wu et al., (2014) expatiated on the effect of misfit dislocation as a major factor that affects electron-hole recombination rate in the LED devices. However, many drawbacks were noticed in the misfit dislocation concept on the account of carrier transport and non-uniform carrier distributions in QDs. The carrier transport in QDs may be expressed via adequate estimation of how carriers either recombine or perform a photo – assisted hopping transition to other localized states [15]. The rate of recombination of localized hole was ab-initio represented mathematically by the listed chain of equations [15]

$$\Gamma_{\sigma}(R) \approx \tau_o^{-1} \exp\left(-\frac{2R}{\alpha}\right) \quad (1)$$

Where  $\Gamma_{\sigma}$  depends on the particular recombination mechanism,  $\alpha$  is the absorption coefficient of the material at the energy of the incoming photon, R is the recombination rate. In the case of radiative recombination shown in figure 1,  $\tau_o$  represent the radiative lifetime of the exciton.

Ref [25] illustrated the tendency charge carrier to perform a non radiative hopping transition especially from an occupied state ‘I’ to an empty localized state j over a distance  $r_{ij}$  is determined by the

$$\Gamma_{i \rightarrow j} = V_o \exp\left[-\frac{2r_{ij}}{\alpha} - \frac{\xi_j - \xi_i + |\xi_j - \xi_i|}{2KT}\right] \quad (2)$$

Where  $\xi_j$  and  $\xi_i$  are the energies of states j and i respectively and  $V_o$  is the attempt- to –escape-frequency of the  $10^{12}s^{-1}$ . Applying the approach of Ref [26], the time of the carrier concentration  $n_k$  in slice number k is determined by the equation

$$\frac{dn_k}{dt} = \sum_{\substack{j=i \\ j \neq k}}^m (n_j \Gamma_{j \rightarrow k} - n_k \Gamma_{k \rightarrow j}) - n_k \Gamma_{\sigma} \quad (3)$$

Where  $\Gamma_{j \rightarrow k}$  is the rate of transition of charge from a state in slice 'j' to a state in slice 'k' and  $\Gamma_{\sigma}$  is the rate of recombination of the charge carriers. It is important to consider the transition rate  $T_{k \downarrow}$  in the device, that is, downward energy from the slice 'k', Ref [15] gave downward transition rate as

$$T_{k \downarrow} = V_o \exp\left(\frac{-2R_k}{\alpha}\right) \quad (4)$$

Where  $R_k$  is the hopping distance determined by energy below  $E_k$ .

$$T_{k \rightarrow j} = V_o \exp\left(\frac{-2R_k}{\alpha}\right) \frac{d_j - n_i(t)}{\sum_{i=k}^m [d_j - n_i(t)]} \quad (5)$$

$$T_{k \rightarrow j} = T_{j \rightarrow k} \frac{d_k - n_k(t)}{d_j - n_i(t)} \exp\left(\frac{\xi_k - \xi_j}{KT}\right) \quad (6)$$

The upward energy transition was also written as

$$T_{k \rightarrow j} = V_o \exp\left(\frac{-2R_k}{\alpha} - \frac{\xi_k - \xi_j}{KT}\right) * \frac{d_j - n_i(t)}{\sum_{i=k}^m [d_j - n_i(t)]} \quad (7)$$

If we consider the concentration of charge carriers at time 't' as 'n', the recombination rate would be of the order  $\Gamma_{\sigma}(n^{-1/2})$ . This means that the recombination rate in equation (3) can be written as the product of the density of filled electron state n and the probability ' $n\alpha^2$ '. This idea is gotten from the filled hole state of a distance  $\alpha$  from filled electron state n.

$$\Gamma_{\sigma} \approx \tau_o^{-1} n(t) \alpha^2 \quad (8)$$

A critical evaluation of equations (1-8) would have been correct via earlier knowledge of lighting device. Recent discovery of the polarization effect via carrier transport and non-uniform carrier distributions in wells have changed the mathematical face of equations (1-8). For example, Ref [13] reported that the c-plane InGaN/GaN devices are subject to large polarization-related electric fields. In this case, the preliminary results were distorted energy band diagram profile with a low electron-hole wavefunction overlap, and low radiative recombination efficiency. This idea is totally different from the theoretical expression highlighted in both the upward and downward transition rates (see equations 6 & 7). As against the carrier transport expressed in equations 6 & 7, polarization effects results in a directionally opposed migration of electrons and holes in the active region. Experimentally, there is a spatial separation of the electron and hole wave functions i.e. leading to a reduced oscillator strength by the quantum-confined Stark effect [27]. This idea may be localized to structures grown along the c-axis orientation i.e. perpendicular to its growth plane [28]. However, the reality of the polarization effect on the photoluminescence (PL) of polar and semi-polar LED (see Figure 4) affirms that the theoretical luminescence spectrum (shown in equation 9) may be obsolete

$$I(\hbar\omega, t) = \alpha \int_{-\infty}^{\infty} n^{(o)}(\hbar\omega + \xi, t) n^{(k)}(\xi, t) d\xi \quad (9)$$

Where  $n^{(o)}(\xi, t)$  and  $n^{(k)}(\xi, t)$  denote the densities of electron and holes respectively. To correct this anomaly, several ideas have been propounded. For example, Ref [28] suggested that the theoretical addition of the strength of internal polarization electric field ( $\xi$  internal) can be estimated at the flat conduction band through

$$\xi_{internal} = \frac{V_{bias}}{d} \tag{10}$$

where  $V_{bias}$  is the voltage applied across the device, and  $d$  is the total thickness of the MQWs active layer region.

Ref [29] also expatiated on the theoretical upgrade of equation (9) via an in-depth explanation of the photoluminescence intensity decay noticed in Figure 4 below. Using equation (11), Ref [29] applied the Boubaker polynomial expansion scheme (BPES) to proffer solutions of the photoluminescence decay intensity at excited states (see figure 5).

$$I_{PL}(x, t) = \int_0^N \cos(kx) \exp(-kt) \Phi(x) dk \tag{11}$$

Where  $\Phi(x)$  is interpreted as an effective decay rate probability density function.  $K$  is the decay rate.

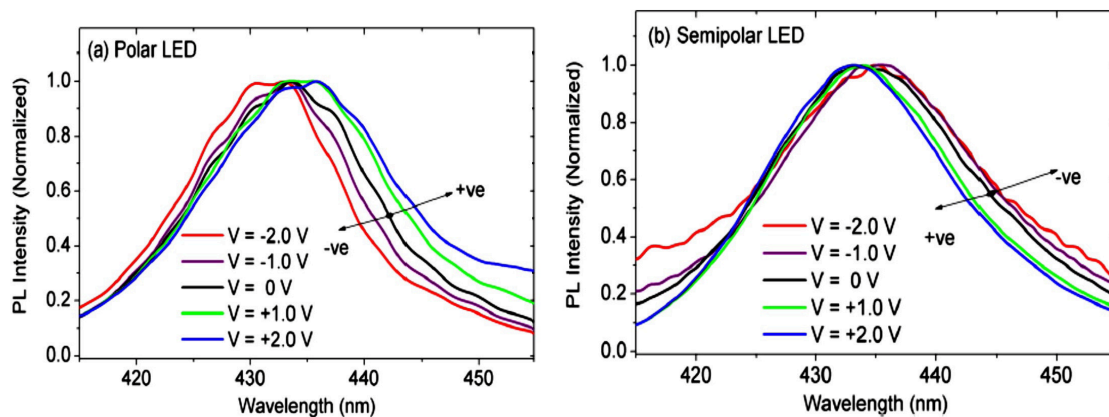


Figure 4: Comparative analysis of polarization effect on photoluminescence spectra of the polar LED device and the semipolar LED device under the external bias from -2 to +2V [13]

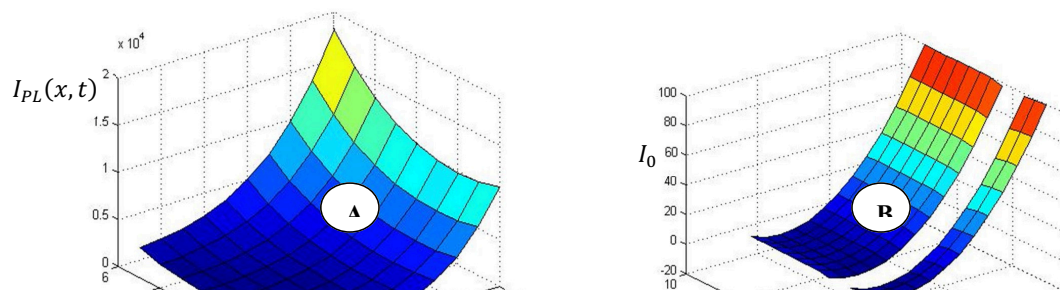




Figure 5 show that  $\phi(k)$  cannot be normalized for certain semiconductor device because of the individual PL decay intensity that depends on the positions of the recombining charges. Salient among the findings of Emetere (2014) was the possibility of realizing one or both radiative and nonradiative relaxation rates from LED devices. Hence, as against the basic understanding of equation 1, some LED devices works on the principles of non-single exponential. The non-single exponential decay could be attributed to more than one type of recombination or trapping centers. Therefore the theoretical comprehension of undesirable influences by polarization fields could be further investigated. Hence, the commercial relevance of the SSL depends on how much physics is resolved based on the non-polar or semi-polar planes [14-15, 30-32].

#### **4. Effect of LED Growing Techniques on its Performance**

The metal-organic chemical vapor deposition (MOCVD) system consists of three-fabrication procedures i.e. growing material in geometrical location i.e. c-plane or r-plane, junction design and doping, and standard device fabrication process. However, the choice on the type of LEDs i.e. blue or red or white LED depends on the desired dimension of sample, junction plane, doping concentration, thickness of buffer layer, deposition flow rate, electrodes (e.g. p-type or n-type), etching technique, basal plane, thermoelectric power factor, type of material (e.g. GaN, substrate), type of polar device (i.e. non-polar and semi-polar), width of active region, and pairs of quantum well (QW) or multiple quantum well (MQW). The physics of combining this entire factor is quite interesting. For example, the buffer layer is used to avoid interference with thermoelectric measurements or extracting thin film thermal conductivities [10]. Few researches have shown that the thickness and type of buffer layer is paramount to filter the amount of interference. For example, Ref [34] showed that a 2  $\mu\text{m}$  thick iron doped semi-insulating buffer layer can be used to filter interference; Nakamura et al., [10] also used 0.03  $\mu\text{m}$  thick GaN buffer layer to minimize interference etc. The growth of the buffer layer depends on the temperature and type of substrate-sapphire, silicon carbide [10]. Chemical vapour deposition is the most widely used technique for depositing many materials in the semiconductor industry. It involves the growth of a solid material from the gas phase using a reactive gas mixture, which supplies the necessary active species.

The stacking of the quantum well (QW) or multiple quantum well (MQW) is used to scrutinize the external and internal quantum efficiency. Extensively, the stacking of either the QW or MQW controls the free hole carrier concentration in either the p-layer or n-layer. It controls the internal absorption of electrodes and epilayer [35]. The stacking of the QW or MQW may follow a three layer approach (see figure 5a), four layer approach (see figure 5b) or beyond five layer approach (see figure 5c&d). Foremost of the plane orientation is the basal plane. Basal plane is used to determine the large built-in electric fields due to spontaneous and piezoelectric polarization in polar LED. Other planes which perform almost same function is the m-plane and the a-plane for non-polar LED, and intermediate plane semi-polar LED. The variation of the basal plane in determining the kind of LED has attracted other physics like critical thickness limit [21,36], basal plane stacking faults (BPSF) etc. BPSFs formation occurs when the QW thickness exceeded 4 nm (Wu et al., 2014) or in m-plane grown samples [37].

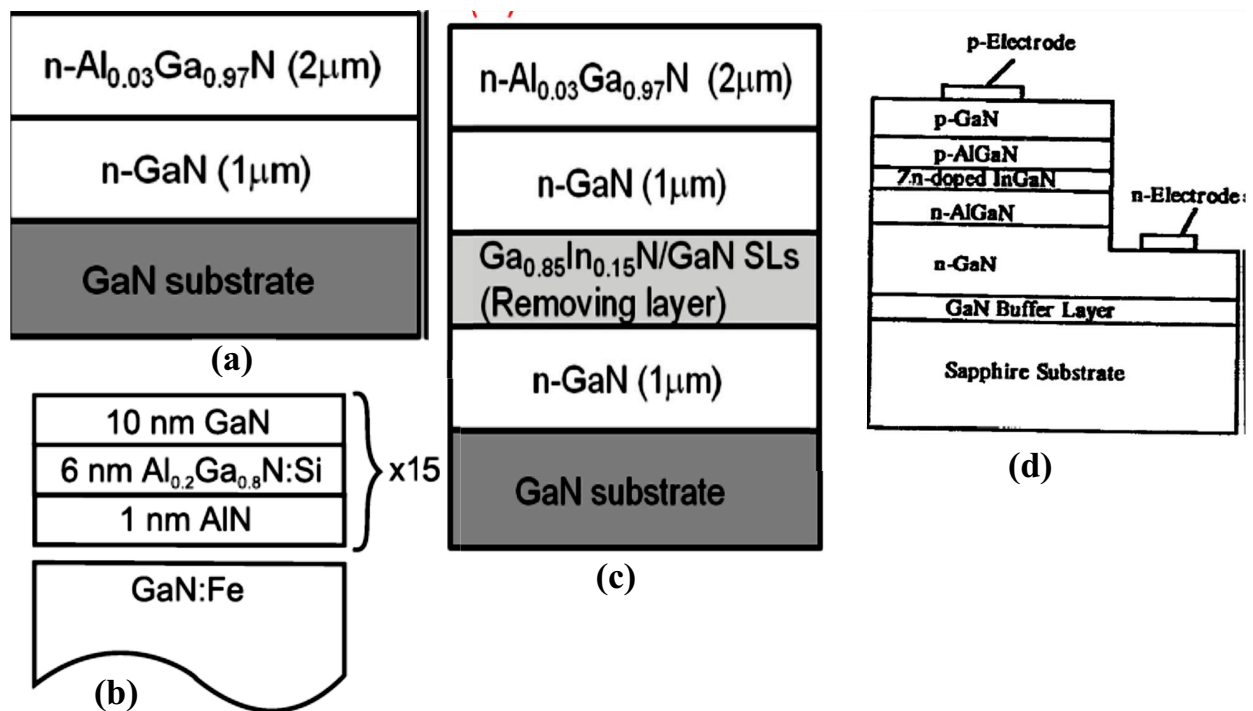


Figure 5: pairing of the quantum well (QW) or multiple quantum well (MQW). a) is the three-layer stacking. b) is the four-layer stacking. c) is the above five-layer stacking

#### 4. Conclusion

To obtain a high colour rendering index, warm light with low colour temperature, high thermal stability and higher energy efficient white LEDs, the physics of the recent discoveries must be understood to understand other technological dynamics of white light LED. The phosphor-free white- light emitters might have taken us close to another technological innovation, however, the ab-initio faults about the theory of the light emitting diode (LED) may plagued its future successes unless something is done.

## Acknowledgements

The authors wish to acknowledge the financial support of host institutions

## Reference

- [1] Kira, M., Jahnke, F., Hoyer, W., & Koch, S., Quantum theory of spontaneous emission and coherent effects in semiconductor microstructures. *Progress in quantum electronics*, 23(6), 189-279, (1999).
- [2] Takagahara, T., Theory of exciton dephasing in semiconductor quantum dots. *Physical Review B*, 60(4), 2638, (1999).
- [3] Uno E. Uno, Moses E. Emetere, Isah K.U and Umaru Ahmadu, On the Effect Of Electron-Hole Recombination In Disordered GaAs-AA<sub>1-x</sub>AlAs Multi-quantum Well Structure. *International Journal of Fundamental Physical Sciences*, 2 (4), 52-57, (2012).
- [4] Min Daehong, Donghwy Park, Jongjin Jang, Kyuseung Lee & Okhyun Nam, Phosphor-free white-light emitters using in-situ GaN nanostructures grown by metal organic chemical vapor deposition. *Sci. Rep.* 5, 17372; doi: 10.1038/srep17372 (2015).
- [5] Huang C. F., Lu C. F., Tang T. Y., Huang J. J., and Yang C. C., Phosphor-free white-light light-emitting diode of weakly carrier-density-dependent spectrum with prestrained growth of InGaN/GaN quantum wells *Appl. Phys. Lett.* 90, 151122 (2007).
- [6] Schubert E. F., Kim J. K., Solid-state light sources *gettingsmart Science* 308, 1274(2005)
- [7] Fujito K., S. Kubo, H. Nagaoka, T. Mochizuki, H. Namita, and S. Nagao, Bulk GaN crystals grown by HVPE, *Journal of Crystal Growth*, 311, 3011-3014 (2009).
- [8] Dal B. Don, K. Kohary, E. Tsitsishvili, S.D. Baranovskii, P. Thomas, and H. Kalt., Quantitative interpretation of the phonon-assisted redistribution processes of excitons in Zn<sub>(1-x)</sub>Cd<sub>x</sub>Se quantum islands. *Phys. Rev. B* 69, 045318, (2004).
- [9] Zhao, Y., Q. Yan, C. Y. Huang, S. C. Huang, P. S. Hsu, S. Tanaka, C. C. Pan, Y. Kawaguchi, K. Fujito, C. G. Van de Walle, J. S. Speck, S. P. DenBaars, S. Nakamura, and D. Feezell, *Appl. Phys. Lett.* 100, 2, (2014)
- [10] Nakamura, S., and M. R. Krames, History of gallium-nitride-based light-emitting diodes for illumination, *Proc. IEEE* 101, 2211 (2013).
- [11] Zhe Zhuang, Yi Li, Bin Liu, Xu Guo, Jiangping Dai, Guogang Zhang, Tao Tao, Ting Zhi, Zili Xie, Haixiong Ge, Yi Shi, Youdou Zheng, and Rong Zhang, Optical polarization characteristics of c-plane InGaN/GaN asymmetric nanostructures, *Journal of Applied Physics*, 118 (23), (2015), 10.1063/1.4938119
- [12] Chih-Feng Lu, Che-Hao Liao, Chih-Yen Chen, Chieh Hsieh, Yean-Woei Kiang, and C. C. Yang, Reduction in the efficiency droop effect of a light-emitting diode through surface plasmon coupling, *Applied Physics Letters*, 96, 261104, (2010)
- [13] Daniel L. Becerra, Yuji Zhao, Sang Ho Oh, Christopher D. Pynn, Kenji Fujito, Steven P. DenBaars and Shuji Nakamura, High-power low-droop violet semipolar (3031) InGaN/GaN light-emitting diodes with thick active layer design, *Applied Physics Letters* 105, 171106, (2014)
- [14] Konar Aniruddha, Amit Verma, Tian Fang, Pei Zhao, Raj Jana and Debdeep Jena, Charge transport in non-polar and semi-polar III-V nitride heterostructures, *Semiconductor Science and Technology*, 27 (2), 024018, (2012).
- [15] Uno E. Uno, Moses E. Emetere, Mathew Aplha., Crystalline Grain Size Effects On The

- Conductivity Of The Doped Tin Dioxide ( $\text{SnO}_2$ ) With Zinc (Zn). *Journal of Ovonic Research*, 10 (3), 83-88, (2014).
- [16] Craven M. D., Lim S. H., Wu F., Speck J. S., and DenBaars S. P., Structural characterization of nonpolar (1 1 2 0) a-plane GaN thin films grown on (1 1 0 2) r-plane sapphire, *Appl. Phys. Lett.*, vol. 81, pp. 469–471, (2002).
- [17] Li, Hongjian, Panpan Li, Junjie Kang, Zhi Li, Zhicong Li, Jing Li, Xiaoyan Yi and Guohong Wang Phosphor-free, colour-tunable monolithic InGaN light-emitting diodes. *Appl. Phys. Express* 6, 102103 (2013).
- [18] Yamamoto S., Zhao Y., Pan C. C., Chung R. B., Fujito K., Sonoda J., DenBaars S. P., and Nakamura S., High-Efficiency Single-Quantum-Well Green and Yellow-Green Light-Emitting Diodes on Semipolar (2021) GaN Substrates, *Appl. Phys. Express* 3, 122102, (2010).
- [19] Enya, Y., Y. Yoshizumi, K. Akita, M. Ueno, M. Adachi, T. Sumitomo, S. Tokuyama, T. Ikegami, K. Katayama, and T. Nakamura, 531 nm green lasing of InGaN based laser diodes on semipolar {20–21} free-standing GaN substrates, *Appl. Phys. Exp.*, vol. 2, 082101, (2009).
- [20] Hardy, M. T., Hsu, P. S., Wu, F., Koslow, I. L., Young, E. C., Nakamura, S., E. Romanov, S. P. DenBaars, and J. S. Speck, Trace analysis of non-basal plane misfit stress relaxation in (20-21) and (30-3-1) semipolar InGaN/GaN heterostructures, *Appl. Phys. Lett.* 100, 202103 (2012).
- [21] Wu, Z. H., Tanikawa, T., T. Murase, Y. Y. Fang, C. Q. Chen, Y. Honda, M., Yamaguchi, H. Amano, and N. Sawaki, Partial strain relaxation by stacking fault generation in InGaN multiple quantum wells grown on semipolar GaN, *Appl. Phys. Lett.* 98, 051902 (2011).
- [22] Anderson, P. W. Localized Magnetic States in Metals. *Phys. Rev.* 124, 41 (1961).
- [23] Uno E. Uno, Moses E. Emeter, Akhpelor A. Ohiozebau, Enebeli C. Benaiah, Onogu A. Williams, Evidence Of Positional Doping Effects On The Optical Properties Of Doped Tin Dioxide ( $\text{SnO}_2$ ) With Zinc (Zn). *Journal of Ovonic Research* 10 (4), 141-147, (2014)
- [24] Yamada Motokazu, Tomotsugu Mitani, Yukio Narukawa, Shuji Shioji, Isamu Niki, Shinya Sonobe, Kouichiro Deguchi, Masahiko Sano and Takashi Mukai, InGaN-Based Near-Ultraviolet and Blue-Light-Emitting Diodes with High External Quantum Efficiency Using a Patterned Sapphire Substrate and a Mesh Electrode, *Jpn. J. Appl. Phys.* 41, L1431 (2002).
- [25] Sedat Nizamoglu, Talha Erdem, Xiao Wei Sun, and Hilmi Volkan Demir, Warm-white light-emitting diodes integrated with colloidal quantum dots for high luminous efficacy and colour rendering, *Optics Letters*, Vol. 35, No. 20 pp 3372-3374, (2010)
- [26] Bando, K., K. Sakano, Y. Noguchi, and Y. Shimiz, Development of High-bright and Pure-white LED Lamps, *J. Light Visual Environ.* 22, 2, (1998).
- [27] Benito Alén, José Bosch, Daniel Granados, Juan Martínez-Pastor, Jorge M. García, and Luisa González, Oscillator strength reduction induced by external electric fields in self-assembled quantum dots and rings, *Physical Review B* 75, 045319, (2007).
- [28] Ji, Y., Z.-H. Zhang, Z. Kyaw, S. T. Tan, Z. G. Ju, X. L. Zhang, W. Liu, X. W. Sun, and H. V. Demir, Enhanced hole transport in InGaN/GaN multiple quantum well light-emitting diodes with a p-type doped quantum barrier, *Appl. Phys. Lett.* 103(5), 053512 (2013).
- [29] Emeter, Moses E., and B. Nikouravan, Femtosecond Spin Dynamics Mechanism

- Probed By the Bloch NMR -Schrödinger Mainframe. *International Journal of Physics & Research* 4(4): 105-110, (2014).
- [30] Daniela Di Martino, Luca Beverina, Mauro Sassi, Sergio Brovelli, Riccardo Tubino & Francesco Meinardi, Straightforward fabrication of stable white LEDs by embedding of inorganic UV-LEDs into bulk polymerized polymethyl-methacrylate doped with organic dyes, *Scientific Reports* 4,4400, (2014).
- [31] Yu Lei, Zhang Yuan-Wen, Li Kai, Pi Hui, Diao Jia-Sheng, Wang Xing-Fu, Hu Wen-Xiao, Zhang Chong-Zhen, Song Wei-Dong, Shen Yue, and Li Shu-Ti, Theoretical analysis of semi/non-polar InGaN/GaN light-emitting diodes grown on silicon substrates, *Chin. Phys. B.* 24 (7), 077801, (2015)
- [32] Yoshida, S., T. Yokogawa, Y. Imai, S. Kimura, and O. Sakata, Evidence of lattice tilt and slip in m-plane InGaN/GaN heterostructure, *Appl. Phys. Lett.* 99, 131909 (2011).
- [33] Mazhar Ali Abbasi, Zafar Hussain Ibupoto, Mushtaque Hussain, Omer Nur and Magnus Willander, The fabrication of white light-emitting diodes using the n-ZnO/NiO/p-GaN heterojunction with enhanced luminescence, *Nanoscale Research Letters* 8, 320, (2013)
- [34] Yamada Motokazu , Takahiro Naitou, Kunihiro Izuno, Hiroto Tamaki, Yoshinori Murazaki, Masatoshi Kameshima and Takashi Mukai, Red-Enhanced White-Light-Emitting Diode Using a New Red Phosphor, *Jpn. J. Appl. Phys.* 42, L20 (2003).
- [35] Takehara, K.K., K. Takeda, S. Ito, H. Aoshima, M. Iwaya, T. Takeuchi, S. Kamiyama, I. Akasaki, and H. Amano, *Jpn. J. Appl. Phys.*, 51, 042101 (2012).
- [36] Matthews, J. W., and A. E. Blakeslee, Defects in epitaxial multilayers I. Misfit dislocations, *J. Crystal Growth*, vol. 27, pp. 118–125, 1974.
- [37] Fischer, A. M., Z. Wu, K. Sun, Q. Wei, Y. Huang, R. Senda, D. Iida, M. Iwaya, H. Amano, and F. Ponce, Misfit Strain Relaxation by Stacking Fault Generation in InGaN Quantum Wells Grown on m-Plane GaN, *Appl. Phys. Express* 2, 041002, (2009).